Transport and Communications Science Journal

CAPTURING MICRO-AMPLITUDE STRUCTURAL VIBRATIONS WITH LOW-COST CAMERAS: A NON-CONTACT MEASUREMENT APPROACH

Le Xuan Luu*, Luong Xuan Binh, Ha Van Quan, Ta Thi Hien

University of Transport and Communications, No 3 Cau Giay Street, Hanoi, Vietnam

ARTICLE INFO

TYPE: Research Article
Received: 04/05/2025
Revised: 13/09/2025
Accepted: 07/11/2025
Published online: 15/01/2026
https://doi.org/10.47869/tcsj.77.1.2

* *Corresponding author*
Email: luusbvl@utc.edu.vn

Abstract. Vibrations of existing structures induced by wind, traffic, and human activities are often ambient in nature. These vibrations typically have low amplitudes, making it challenging to capture their motion with a camera. This paper presents a framework for measuring the displacement of structural ambient vibrations without physical contact using a low-cost camera. The micro-amplitude vibrations of the structure are captured by the camera and then amplified using the Phase-Based Video Motion Magnification (PVMM). The centroid of structural target segments in each image frame is tracked using the proposed Shape-Box Tracking (SBT). Unwanted background objects are removed using the proposed Line-Based Color Selection (LCS). Vibration characteristics are determined using frequency-based analysis and Random Decrement Technique (RDT). Two experiments based on the proposed framework were conducted to demonstrate its effectiveness. The first involved free-decay vibration testing with large amplitudes, while the second focused on ambient vibration with small amplitudes, emphasizing motion magnification. The success of this method paves the way for applying low-cost cameras in the operational measurement of existing structures.

Keywords: Computer vision; non-contact measurement; low-cost camera.

1. INTRODUCTION

Vibrations in existing civil structures, such as bridges, buildings, and towers, are frequently induced by naturally occurring or operational forces such as wind, road traffic, pedestrian movement, and nearby machinery. These excitations are typically ambient in nature, meaning they are random, broadband, and not generated through controlled input. Ambient vibration monitoring plays a crucial role in structural health assessment, enabling the extraction of key dynamic characteristics such as natural frequencies, mode shapes, and damping ratios. These parameters are essential for identifying changes in structural integrity, detecting damage, or updating numerical models. Since ambient excitation is low in amplitude and often spatially distributed, it presents a challenge for traditional measurement methods that rely on high-sensitivity contact sensors or labor-intensive test setups.

Conventional measurement methods have relied heavily on contact-based sensors such as accelerometers [1, 2], wireless sensors [3], to measure dynamic responses and detect early signs of structural degradation. While effective, these methods often involve high installation and maintenance costs, require direct access to the structure, and may introduce mass-loading effects that influence the natural frequencies of structures. As a result, non-contact measurement methods, such as laser vibrometers [4] have emerged as a promising alternative, enabling remote assessment of structural vibrations without physical access to the structures. These methods are particularly attractive for monitoring large-scale or difficult-to-access structures, such as bridges, towers, or heritage buildings.

Vision-based methods, particularly those employing video cameras, have recently become a promising non-contact approach for structural vibration measurement. This approach offers several advantages: ease of deployment, the ability to capture motion at multiple points simultaneously, and the potential to assess large or hard-to-access structures, such as long-span bridges or heritage buildings [5]. Feng et al. [6] introduced a subpixel orientation code matching (OCM) algorithm to enhance accuracy, and Jana and Nagarajaiah [7] developed a real-time monitoring approach using a handheld camera. A wide range of studies have demonstrated the potential of computer vision-based vibration measurement [8, 9, 10, 11].

However, measuring ambient structural vibrations using cameras, especially low-cost ones remains challenging due to the typically low amplitude of these vibrations. For micro-scale vibrations, it is difficult for cameras to accurately detect and extract meaningful motion signals. Additionally, the presence of unwanted objects in the image background often complicates the identification of the target structure. Although low-cost camera such as smartphone camera are usually affordable, the image processing with its video is usually difficult, especially when capturing micro structural vibrations. Therefore, developing a framework that enables the use of low-cost cameras to capture structural vibrations and process image data is critically important. In a recent study [5], the authors proposed a stereo vision-based vibration measurement method using a synchronized multi-camera setup combined with video motion magnification. Although this approach successfully captured three-dimensional vibrations of cables, it relied on expensive equipment, and challenges related to background interference remained unaddressed.

In this paper, the authors propose a framework for measuring micro-vibrations of line-like structures with a low-cost camera (e.g., a smartphone camera), while accounting for interference from non-structural background objects. Specifically, micro-amplitude structural vibrations are recorded by the camera and subsequently amplified through a PVMM technique. The structural target segments are identified in each video frame using the proposed SBT

method, and unwanted background elements are eliminated through the proposed LCS algorithm. Vibration characteristics are then extracted via frequency-based analysis and the RDT. Experimental validation confirms the effectiveness of the proposed method, highlighting its potential for low-cost, non-contact structural monitoring in real-world applications.

2. METHODOLOGY

Low-cost cameras, such as consumer-grade webcams, smartphones, or entry-level digital cameras, offer a compelling alternative to high-end imaging systems for structural vibration measurement. This section presents a framework for measuring the vibrations of line-like structures using a single low-cost camera, enhanced by a developed image processing package. The framework enables the extraction of time-history displacement signals and the identification of key vibration characteristics, including natural frequencies and damping ratios. The proposed methodology comprises five main steps: Step 1. Video acquisition and camera setup: Structural vibrations are recorded using a low-cost camera; Step 2. Background elimination: Unwanted non-structural elements in the video are eliminated using the proposed LCS algorithm; Step 3. Motion magnification: Micro structural vibrations are magnified using the PVMM technique; Step 4. Displacement extraction: Time-domain displacements are extracted from magnified video using the proposed SBT method; Step 5. Vibration analysis: The vibration characteristics are determined through frequency-domain analysis and the RDT.

2.1. Video acquisition and camera setup

In the first step of the proposed framework, structural vibrations are recorded using a low-cost camera. The camera is positioned to face the target structure ensuring a clear and unobstructed line of sight. To minimize the effects of camera shake or external disturbances, the device is securely mounted on a tripod or other rigid support. When using a smartphone camera, it is important to avoid physically touching the phone to initiate recording, as this can introduce motion artifacts. Instead, the use of a wireless remote control or a synchronized external trigger is recommended to start video capture without disturbing the setup. Regarding camera settings, the frame rate should be selected based on the Nyquist criterion [12], which states that the sampling frequency must be at least twice the highest structural vibration frequency of interest (i.e., $f_{camera} > 2 \times f_{structure}$). However, for improved accuracy particularly when using image processing techniques, it is advisable to use the highest frame rate available to ensure sufficient temporal resolution for capturing micro-amplitude vibrations.

2.2. Proposed Line-Based Color Selection algorithm

The proposed LCS algorithm is designed to isolate structural elements in a video frame by identifying their characteristic color. In computer vision, an image is represented as a 3D array where each pixel has an RGB (Red, Green, Blue) value corresponding to its color. As shown in Fig.1, the LCS method begins by defining a region of interest (ROI) on the structural segment. A line is manually drawn along this segment, and the RGB values of the pixels along this line are extracted. The average of these RGB values is computed to define the target color of the structure.

$$R_t = \frac{\left(R_1 + R_2 + ... + R_n\right)}{n}; G_t = \frac{\left(G_1 + G_2 + ... + G_n\right)}{n}; B_t = \frac{\left(B_1 + B_2 + ... + B_n\right)}{n} \quad (1)$$

in which, R_t, G_t and B_t represent the target RGB color components of the structural segment in the Red, Green, and Blue channels, respectively. These values are obtained by averaging the

individual RGB components (R_i, G_i, B_i) of n pixels sampled along the user-selected line on the structure. To eliminate background and non-structural elements, the algorithm compares every pixel in the frame to the target color (Eq. 2). If a pixel's color is within a predefined threshold (tolerance) of the target RGB value, it is retained (Eq. 3). Otherwise, it is replaced with a background color (usually black), effectively filtering out irrelevant features.

$$\Delta R_i = \left(R_i - R_t\right); \Delta G_i = \left(G_i - G_t\right); \Delta B_i = \left(B_i - B_t\right) \quad (2)$$

$$\Delta_i = \sqrt{\Delta R_i^2 + \Delta G_i^2 + \Delta B_i^2} \le \varepsilon \quad (3)$$

where, Δ_i represents the difference between colors at a given point and target colors; and, ε is tolerance. This process ensures that only the structural segment of interest remains visible in the frame, enabling more accurate displacement tracking and vibration analysis in subsequent steps.

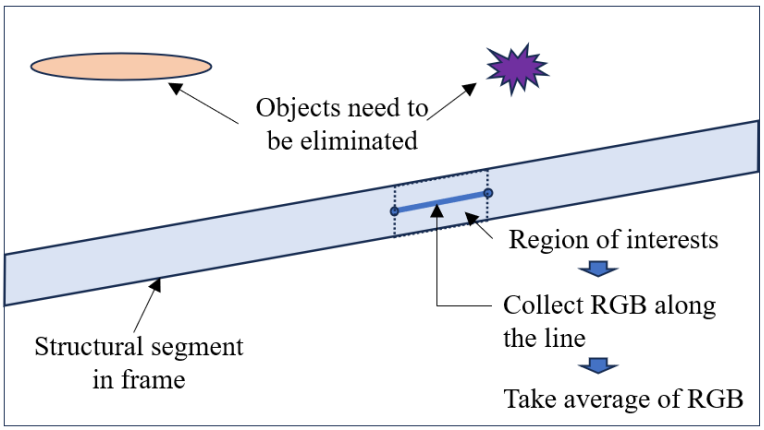

Figure 1. Demonstration of Line-Based Color Selection (LCS) algorithm.

2.3. Phase-Based Video Motion Magnification technique

After unwanted objects are eliminated from the background of the images, the PVMM is used to amplify subtle motions. Originally introduced by Wadhwa et al. [13], the PVMM analyzes temporal variations in the phase information of video frames rather than relying solely on pixel intensity changes. Unlike traditional motion tracking methods, which may struggle with noise or low-amplitude movements, the PVMM leverages a multi-scale, multi-orientation decomposition using a complex steerable pyramid filter. This allows the algorithm to separate local phase and amplitude components within an image sequence. The local phase signals, which encode structural motion, are filtered to isolate specific frequency bands, amplified by a chosen factor, and then recombined with the original amplitude to reconstruct a motion-magnified video. This technique is particularly effective for visualizing micro-scale vibrations in civil engineering applications. For a detailed explanation of the algorithm, readers are referred to the original publications by Wadhwa et al. [13, 14].

A concise outline of the mathematical basis is given below. Each video frame can be expressed using a Fourier series expansion as a combination of complex sinusoidal terms

$$I\left(x+\delta\left(t\right)\right) = \sum_{\omega=-\infty}^{\infty} A_\omega e^{i\omega\left(x+\delta(t)\right)} \quad (4)$$

in which, $I(x+\delta(t))$ is the image intensity, x is the spatial coordinate (image coordinate), $\delta(t)$ denotes the temporal displacement function, A_ω is the amplitude for frequency ω, $i^2 = -1$, and $\omega(x+$

$\delta(t)$) encodes the motion information. By modifying this phase, the motion can be manipulated. Firstly, the phase is first filtered to retain only the desired temporal frequency components, then multiplied by an amplification factor α to magnify motion as

$$I\left(x+\left(1+\alpha\right)\delta\left(t\right)\right)=\sum_{\omega=-\infty}^{\infty}A_{\omega}e^{i\omega\left(x+\left(1+\alpha\right)\delta\left(x,t\right)\right)} \tag{5}$$

Finally, the motion-magnified video is reconstructed by collapsing the pyramid, i.e., recombining all sub-bands into a single video within the selected frequency range. The target frequency band should coincide with the natural frequency of the structure. The amplification factor α plays a decisive role: higher values enhance motion visibility but may also increase noise and visual distortion.

2.4. Proposed Shape-Box Tracking method

This step aims to pinpoint the centroids of the structural segments. Since non-structural objects have been removed from the background, the resulting binary image contains only the target structural segment. Tracking the centroid of this segment across frames allows for the extraction of its time-history displacement. The centroid extraction process relies on geometric property analysis. Geometric properties refer to measurable attributes of objects (typically white regions on a black background), such as shape, size, and position. These properties are critical for motion and displacement tracking. The first step involves determining the orientation axis of the object. Fig. 2 illustrates the orientation axis of an object in a binary image.

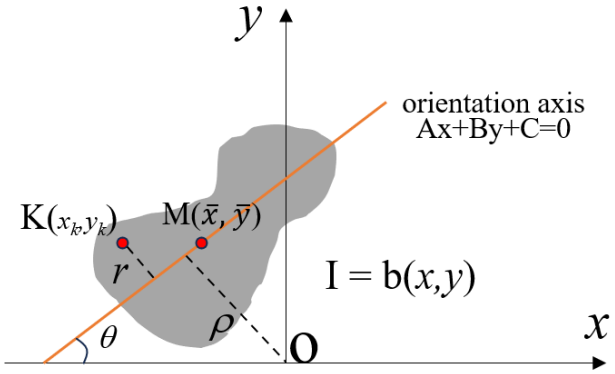

Figure 2. Geometric properties and orientation axis of the object.

The orientation axis is calculated based on the principle of the least second moment of area. In other words, the second moment of the object is computed with respect to a candidate orientation axis, and the orientation angle θ that minimizes this moment is selected. The second moment E with respect to an orientation axis is defined as:

$$E=\iint_{I}r^{2}b\left(x,y\right)dxdy \tag{6}$$

where $b(x,y)$ is the characteristic function, equal to 1 for points within the object and 0 outside, and r is the perpendicular distance from a point (x,y) to the orientation axis. For a general line $Ax+By+C=0$, the distance r from a point $\mathrm{K}(x_k,y_k)$ to the line is given as:

$$r=\left|\frac{Ax_{k}+By_{k}+C}{\sqrt{A^{2}+B^{2}}}\right| \tag{7}$$

Having $x\sin\theta-y\cos\theta+\rho=0$, the distance becomes $r=|x\sin\theta-y\cos\theta+\rho|$. Substituting r into eq.(6) gives

$$E=\iint_{I}\left(x\sin\theta-y\cos\theta+\rho\right)^{2}b\left(x,y\right)dxdy \tag{8}$$

By shifting the coordinate to the centroid M($\bar{x}$, $\bar{y}$) and defining $x' = x - \bar{x}; y' = y - \bar{y}$, eq. (8) transforms into

$$E = a\sin^2\theta - b\sin\theta\cos\theta + c\cos^2\theta \tag{9}$$

where, $$a = \iint_{I'} (x')^2 b(x,y)\,dx'dy'; b = 2\iint_{I'} (x'y')b(x,y)\,dx'dy'; c = \iint_{I'} (y')^2 b(x,y)\,dx'dy'$$

.Minimizing eq. (9) with respect to θ gives the orientation angle

$$\tan 2\theta = \frac{b}{a-c} \tag{10}$$

Once the orientation angle is known, a bounding box aligned with the object's axis can be constructed around the structural segment. This box is centered on a selected point typically the centroid and used to track the segment's motion frame by frame, providing the time-history of the segment's displacement. The proposed SBT method offers several advantages over conventional centroid or contour/feature-based tracking approaches. Traditional centroid tracking often assumes a fixed orientation and can be affected by background noise, while contour or feature-based methods may require complex computations and are sensitive to texture or illumination variations. In contrast, the SBT uses the orientation axis of the structural segment to construct a bounding box aligned with the object's shape. This alignment improves robustness against background interference and geometric distortion, ensuring more stable displacement extraction for line-like structures.

2.5. Vibration analysis

The time-history displacement data of vibrating structural segments is now used to determine their vibration characteristics, specifically the natural frequencies and damping ratios. While natural frequencies can be identified using frequency-domain methods such as the Fast Fourier Transform (FFT), the damping ratio is determined using the RDT. The RDT is a robust time-domain method for extracting modal properties from vibration signals recorded under ambient or unknown excitations. It has been widely applied in civil, mechanical, and aerospace engineering due to its ability to analyze dynamic behavior without requiring input force measurements [15]. The RDT is developed based on the fact that a random vibration is the combination of a deterministic part (due to initial displacement and initial velocity) and a random part (due to random excitation). If $y(t)$ denotes the random response, its free-decay component $y_0(t)$ can be obtained by averaging N equally spaced segments of length τ.

$$y_0(t) = \frac{1}{N}\sum_{i=1}^{N} y(t_i + \tau) \tag{11}$$

Through this averaging process, the random portion of the response is cancelled out, leaving only the deterministic free-decay signal, which corresponds to the homogeneous solution of the structure's equation of motion. Once $y_0(t)$ is obtained, the damping ratio ξ can be evaluated using the logarithmic decrement method:

$$\xi \approx \frac{\delta}{2\pi} = \frac{1}{2\pi\kappa}\ln\frac{y_0(t)}{y_0(t+\kappa T)} \tag{12}$$

where $y_0(t)$ and $y_0(t + \kappa T)$ are the amplitudes of decaying responses at time t and $t + \kappa T$, T is period (s), and κ is the number of successive peaks.

3. EXPERIMENTAL VALIDATION

3.1 Purpose and Experimental setup

To validate the feasibility and applicability of the proposed method to structural systems, two experiments were conducted. The first experiment involved free-decay vibration testing with large motion amplitudes, while the second focused on ambient vibration with small motion amplitudes. In the first experiment, the background contained no unwanted objects, only the structure itself was present. Since the vibration amplitudes were large, there was no need to apply the PVMM. Time-history displacements obtained from the low-cost camera were compared with those measured by a conventional displacement transducer to validate the accuracy of the results. In the second experiment, the background included non-structural objects, and the vibration amplitudes were small due to ambient excitation. To address this, the proposed LCS algorithm was applied to eliminate unwanted background objects, and the PVMM was used to magnify the subtle structural vibrations. Fig. 3 illustrates the experimental setup. The beam was made of steel with an elastic modulus $E = 2 \times 10^5$ Mpa. It had a length l = 78.0 cm, and a rectangular cross-section with a width b = 4.0 cm and a height h = 0.8 cm. For validation, a displacement transducer was installed 18.0 cm from the free end of the beam to measure real-time displacements, which were then compared with the displacements captured by the low-cost camera. The tested beam with a length-to-depth ratio is sufficient to be treated as a beam member. The measurement point was placed away from the clamped end so that, according to Saint-Venant's principle, the influence of boundary conditions on the recorded response is negligible. The same beam specimen was used for both the free vibration and the ambient vibration tests to ensure consistency in the experimental program. The experiments were conducted under normal laboratory electric lighting without the use of controlled lighting equipment.

The camera used was a Redmi Note 11S, operating at 30 frames per second (fps) with a resolution of 1920 × 1080 pixels. The smartphone was mounted on a tripod during the recording process. The smartphone camera was placed at a distance of about 120 cm from the beam, aligned perpendicular to its axis, and firmly mounted on a tripod to minimize lens distortion and perspective effects. A remote control was used to start and stop the video recording to ensure the camera remained stable during measurements.

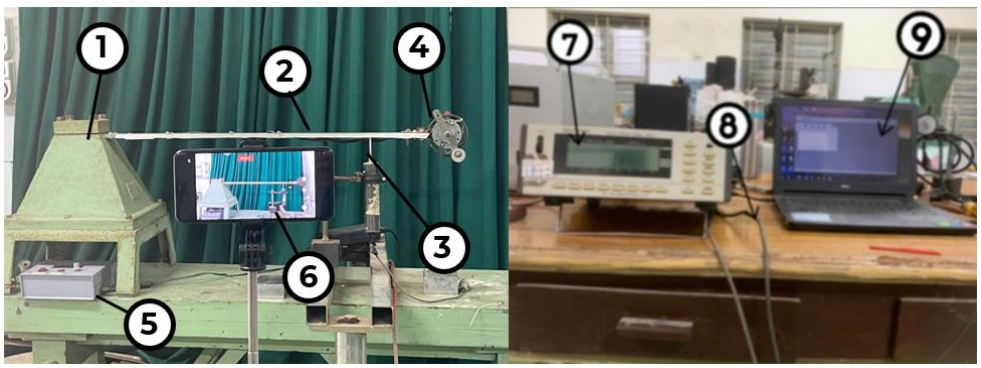

Figure 3. Experiment setup for displacement measurement of beam. Note: 1) Fixed support; 2) Beam; 3) Dynamic displacement transducer; 4) Motor for ambient excitation; 5) Motor speed controller; 6) Low-cost camera (cellphone); 7) Dynamic data logger - SDA 830C type; 8) Signal cable connecting the displacement transducer to the data logger; 9) Computer for data acquisition.

3.2 Free vibration test

For the free vibration test, the beam was initially excited and then allowed to vibrate freely after the excitation was released. A smartphone camera recorded the vibration of the entire beam at a frame rate of 30 frames per second (fps), resulting in 225 image frames extracted from the video as shown in Fig. 4 (this dataset was sufficient to extract stable displacement signals and identify the natural frequency and damping ratio). A 5 × 15 grid was overlaid on each frame to facilitate the selection of the target segment. In this test, the 12th column segment was selected, which also corresponds to the location of the displacement transducer (Fig. 5). The centroid of this segment was tracked over time, providing time-history displacement data of the beam at the transducer's location. Fig. 6 compares the time-domain displacement of the beam measured by the camera with that obtained from the conventional transducer. The results show good agreement between the two methods. Figs. 7 and 8 compare the natural frequency and damping ratio determined using the proposed vision-based method with those obtained from the transducer. Using the conventional transducer, the beam's natural frequency and damping ratio were found to be 5.61 Hz and 0.80%, respectively. The proposed vision-based method estimated them as 5.7 Hz and 0.88%, respectively. These results demonstrate that the vision-based approach yields vibration characteristics that are in good agreement with those obtained from traditional transducers. A frequency deviation of less than 2% was observed compared to conventional displacement transducers. It is noted that a smartphone camera (30 fps, 1920 × 1080 resolution) was used and firmly mounted on a tripod with remote control to avoid camera shake. These recording conditions ensured stable acquisition, allowing reliable comparison with conventional displacement transducers.

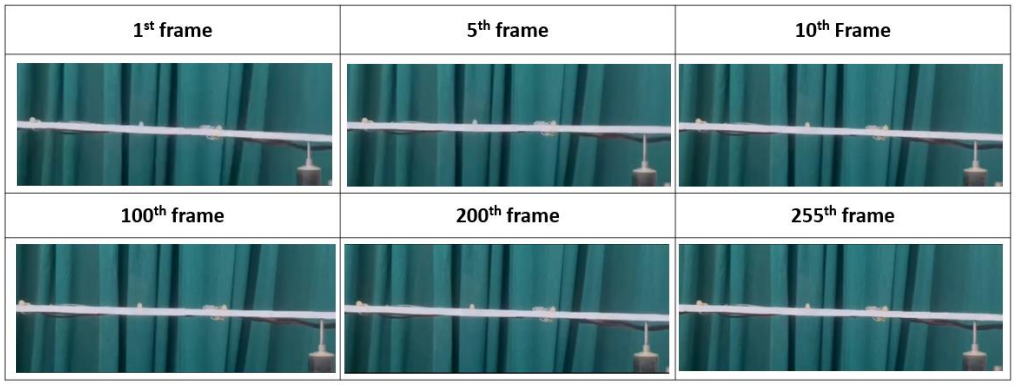

Figure 4. Image frames extracted from camera.

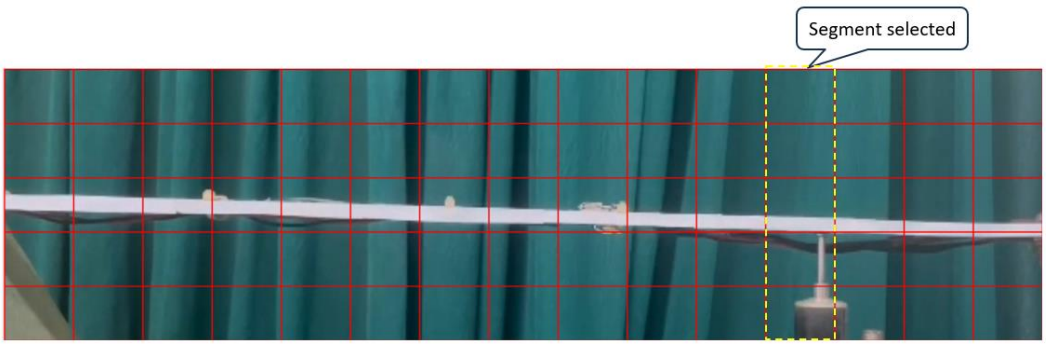

Figure 5. Segment selected for analysis.

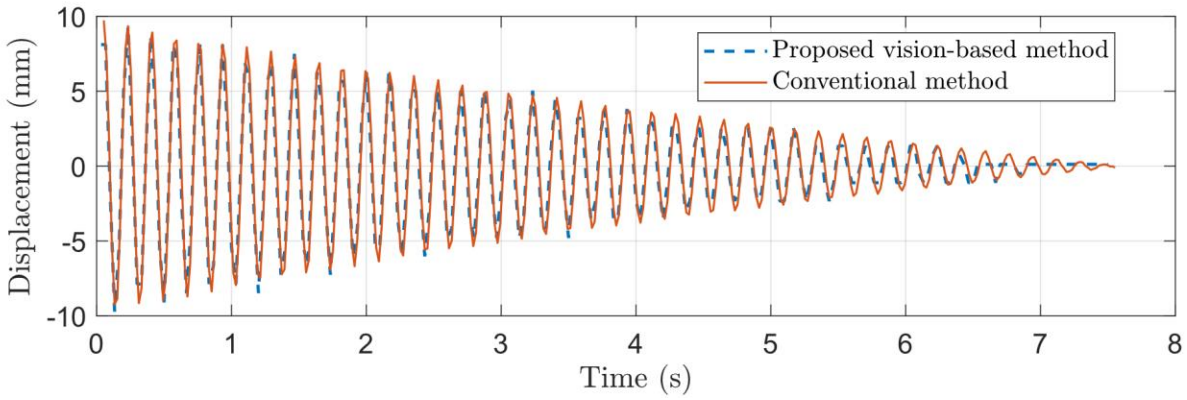

Figure 6. Compare time-history displacements of beam between proposed vision-based method and conventional method.

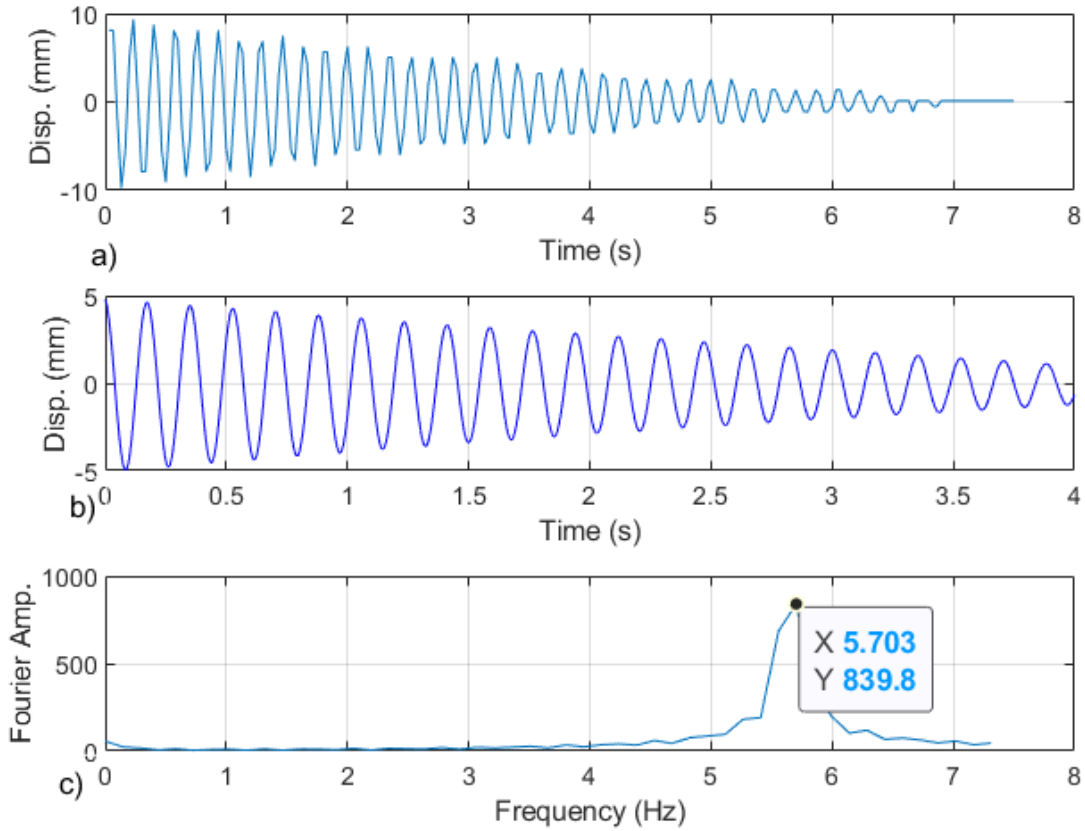

Figure 7. Frequency and damping identification obtained by proposed vision-based approach: a) Raw data; b) Random Decrement (RD) results; c) Frequency Spectrum of RD.

To quantitatively assess the accuracy of the proposed vision-based measurement method, the displacement time-history obtained from the camera was compared with that recorded by the conventional displacement transducer. Three statistical indicators were used: 1) Correlation coefficient *r* (Eq. 13); 2) Root Mean Square Error *RMSE* (Eq. 14); và 3) Relative error *Error* (Eq. 15).

$$\rho(A,B)=\frac{1}{N-1}\sum_{i=1}^{N}\left(\frac{A_i-\mu_A}{\sigma_A}\right)\left(\frac{B_i-\mu_B}{\sigma_B}\right) \tag{13}$$

in which, N is number of data points; μ_A and σ_A are the mean and standard deviation of data A (displacement measured by camera), respectively; and, μ_B and σ_B are the mean and standard deviation of data B (displacement measured by displacement transducer).

$$RMSE=\sqrt{\frac{\sum_{i=1}^{N}(A_i-B_i)^2}{N}} \tag{14}$$

$$Error=\frac{RMSE}{\max(B_i)}\times 100 \tag{15}$$

From the experimental data, the following values were obtained: Correlation coefficient ρ of 0.98, *RMSE* is 0.80 mm, and Relative error *Error* is 8.25%. The correlation coefficient close to unity demonstrates that the proposed vision-based method reliably reproduces the waveform and phase of the structural vibration. This confirms that the dynamic characteristics were captured with high fidelity. The RMSE value of approximately 0.8 mm corresponds to about 8% of the actual vibration amplitude. This indicates that while the camera-based approach accurately represents the temporal evolution of the vibration, it slightly underestimates the displacement amplitude. Such deviation may arise from pixel-to-millimeter calibration errors, sub-pixel tracking limitations, residual timing interpolation, or noise amplification introduced by image-processing techniques. Overall, the results confirm that the proposed vision-based measurement system achieves good agreement with the conventional contact transducer.

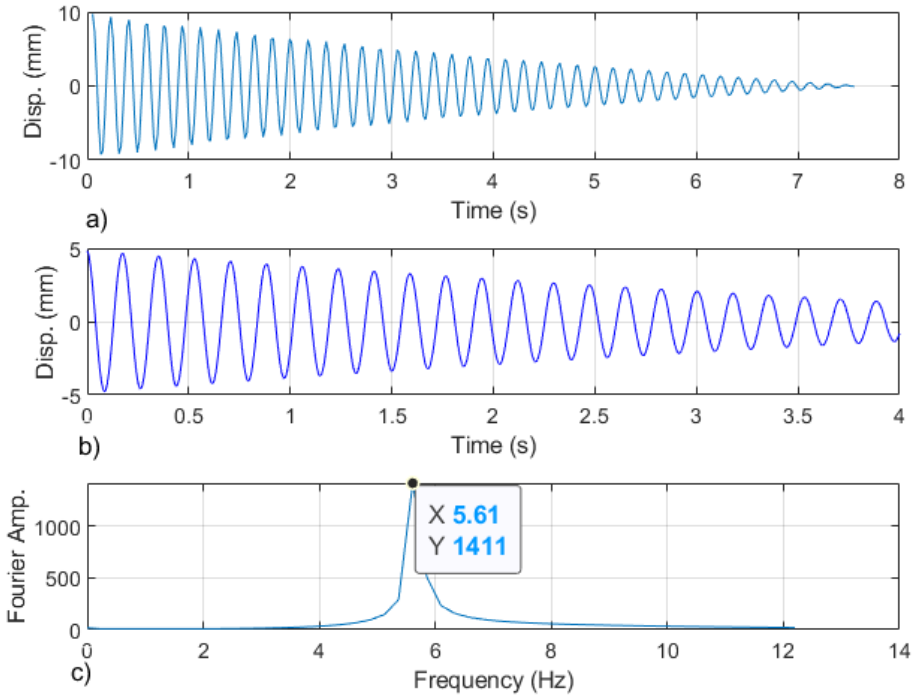

Figure 8. Frequency and damping identification obtained by conventional transducer: a) Raw data; b) Random Decrement (RD) results; c) Frequency Spectrum of RD.

3.3 Ambient vibration test

In this ambient vibration test, an artificial object was placed behind the beam (Fig. 9), and the beam was excited by ambient vibrations generated by a motor. First, the proposed LCS algorithm was applied to remove unwanted structural objects from the background. Based on the sensitivity analysis conducted in this experiment, a tolerance of 50 in RGB values was found to provide stable performance for the steel beam under laboratory lighting conditions (Fig. 10); then, the PVMM was used to magnify the micro-vibrations. With the PVMM being used in this experiment, the amplification factor α of 100 was selected empirically to ensure that the structural vibration was clearly visible while minimizing noise amplification (see the magnified video here: https://drive.google.com/file/d/15nkNMhPcp4NkXt9POeN3B7usWTk5zzt9/view?usp=drive_link). The magnified video was subsequently used to track the displacement of the beam at a selected location. The displacement tracking is shown in Fig. 11, where unwanted objects were removed, and the background was changed to black (corresponding to RGB(0,0,0)). The time-history displacement of the beam was then used for frequency-domain analysis to determine the beam's natural frequency. The FFT results in Fig. 12 show a natural frequency of 5.6 Hz, which is similar to the value determined from the free vibration test. The results of this experiment demonstrate that the proposed vision-based displacement framework enables the use of low-cost cameras, such as smartphone cameras, to measure not only large motion but also ambient motion of line-like structures. It also successfully removes non-structural elements from the background.

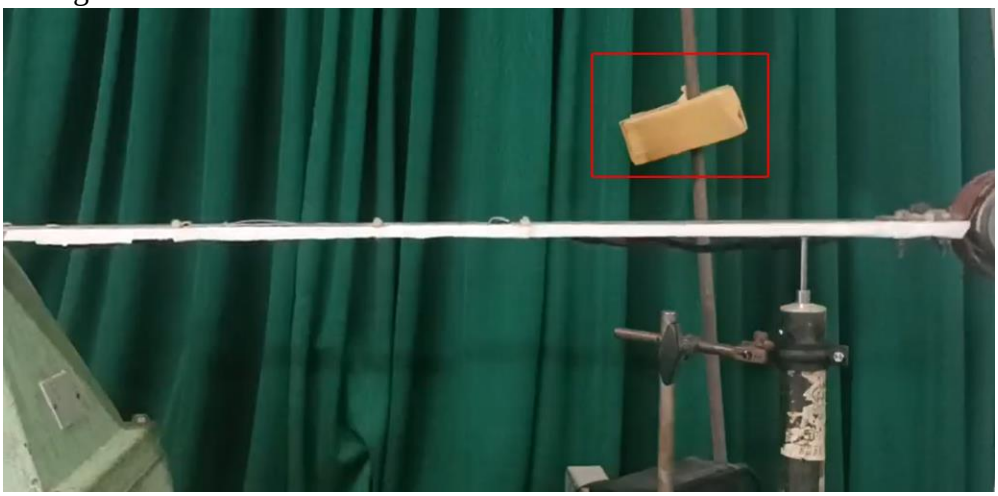

Figure 9. Ambient vibration test with unwanted objects in the background.

a) b) c)

Figure 10. Sensitive investigation on the tolerance of the LCS algorithm: a) tolerance of 5; b) tolerance of 50; tolerance of 100.

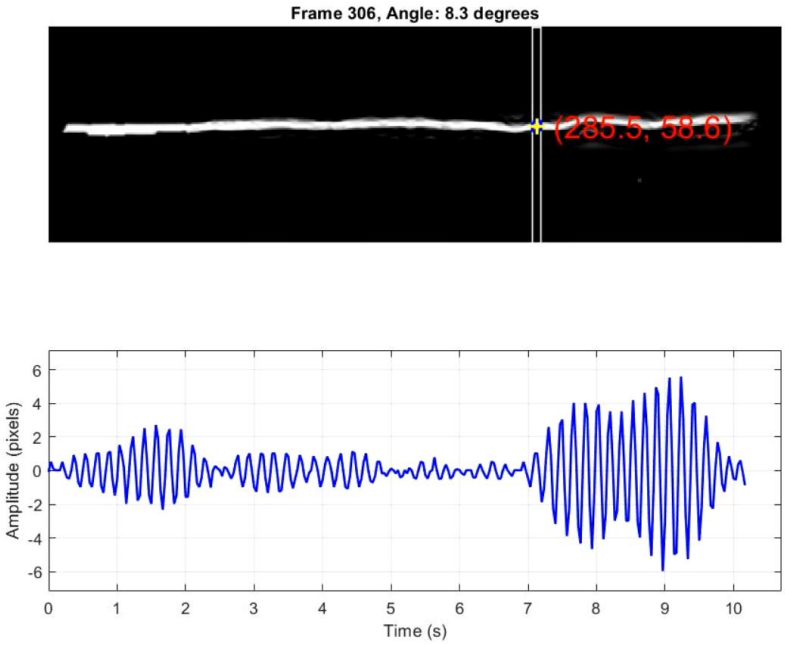

Figure 11. Time-history displacement of the beam obtained using the LCS algorithm and the PVMM method.

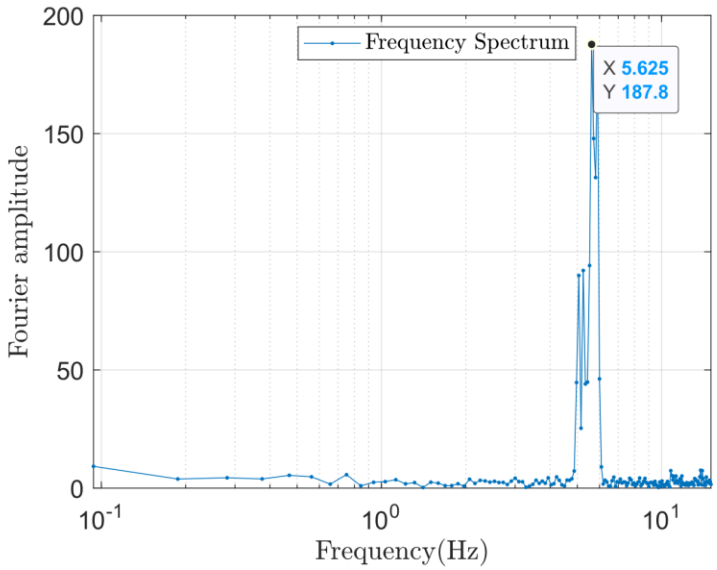

Figure 12. Frequency domain analysis of the ambient vibration data.

4. DISCUSSION ON PRACTICALITY AND LIMITATIONS OF THE PROPOSED METHOD

This study validated the proposed framework under laboratory conditions. The practical implementation of the proposed framework demands careful consideration of several key factors:

- The measurement in outdoor environments, especially rainy weather, remains to be examined. Rain may alter surface appearance and introduce transient artifacts that affect color-based segmentation. Future work will address these challenges by exploring motion/frequency-based filtering to suppress rain-induced noise while preserving vibration signals.
- For practical applications to real structures, camera settings must be carefully considered. According to the Nyquist criterion, the frame rate should be at least twice the highest target frequency of the structure. The resolution should be sufficient to clearly capture the structural segment of interest, and camera stability must be maintained using rigid supports. Future studies will systematically investigate the influence of fps, resolution, and recording conditions on measurement accuracy, particularly in outdoor environments.
- Ensuring camera stability is also critical to avoid unintended motion caused by external factors such as traffic or wind. The camera should be firmly mounted on a tripod or rigid support. If camera vibration becomes significant, the quality of the recorded video may be compromised. In such cases, additional countermeasures can be applied, for example, incorporating fixed reference points within the same video frame to separate camera motion from structural vibration, or applying image stabilization and motion compensation algorithms to correct for global frame shifts.
- With a 30 fps smartphone camera, vibrations up to about 15 Hz can be reliably captured, which is sufficient for most large-scale civil structures whose fundamental frequencies are typically low. However, higher frame rate cameras are required when investigating higher-order vibration modes.
- The required measurement duration depends on the purpose of analysis: a short recording capturing several vibration cycles is sufficient for identifying fundamental dynamic characteristics, while longer recordings may be needed for multi-mode or non-stationary responses. Also, a single well-controlled laboratory trial gave stable results, but field applications may require repeated tests and statistical analysis for reliability

5. CONCLUSIONS

The proposed framework for measuring structural ambient vibrations using low-cost cameras provides a reliable, non-contact solution for monitoring micro-amplitude vibrations in structures. This study proposes the LCS to remove unwanted background elements and the SBT to track the displacement of structural segments over time. For ambient vibrations, the method employs the PVMM to amplify vibration amplitudes. The time-history displacement data obtained from the vision-based method were validated against measurements from conventional transducers, confirming the accuracy and effectiveness of the approach in identifying vibration characteristics. This work highlights the potential of low-cost cameras, such as smartphones, as practical tools for structural health monitoring in both research and real-world applications. Future efforts will focus on further optimizing the framework and extending its applicability to a broader range of structural types, including outdoor environments.

ACKNOWLEDGMENT

This research is funded by University of Transport and Communications (UTC) under grant number T2025-CT-029.

REFERENCES

[1]. L.X. Le, H. Katsuchi, S. Kawai, Damping in stay cable with damper: Practical universal damping curve and full-scale measurement, Journal of Sound and Vibration, 569 (2024) 118090. https://doi.org/10.1016/j.jsv.2023.118090
[2]. X. Le, H. Katsuchi, B. Luong, L. Vu, Q. Ha, Enhancing vibration control in stay cables: A modified damping formulation with NS-HDR damper, Transport and Communications Science Journal, 75 (2024) 1198-1212. https://doi.org/10.47869/tcsj.75.1.8
[3]. Y. Fujino, D.M. Siringoringo, Recent research and development programs for infrastructures maintenance, renovation and management in Japan, Structure and Infrastructure Engineering, 16 (2020) 3-25. https://doi.org/10.1080/15732479.2019.1650077
[4]. A.B. Mehrabi, S. Farhangdoust, A laser-based noncontact vibration technique for health monitoring of structural cables: background, success, and new developments, Advances in Acoustics and Vibration, 1 (2018) 8640674. https://doi.org/10.1155/2018/8640674
[5]. L.X. Le, D.M. Siringoringo, H. Katsuchi, Y. Fujino, B.X. Luong, Stereovision-based vibration measurement of stay cable using synchronized multi-camera setup and video motion magnification, Engineering Structures, 296 (2023) 116938. https://doi.org/10.1016/j.engstruct.2023.116938
[6]. D. Feng, T. Scarangello, M.Q. Feng, Q. Ye, Cable tension force estimate using novel noncontact vision-based sensor, Measurement, 99 (2017) 44-52. https://doi.org/10.1016/j.measurement.2016.12.020
[7]. D. Jana, S. Nagarajaiah, Computer vision-based real-time cable tension estimation in Dubrovnik cable-stayed bridge using moving handheld video camera, Structural Control and Health Monitoring, 28 (2021) e2713. https://doi.org/10.1002/stc.2713
[8]. Y. Shao, L. Li, J. Li, S. An, H. Hao, Computer vision based target-free 3D vibration displacement measurement of structures, Engineering Structures, 246 (2021) 113040. https://doi.org/10.1016/j.engstruct.2021.113040
[9]. K. Luo, X. Kong, J. Zhang, J. Hu, J. Li, H. Tang, Computer vision-based bridge inspection and monitoring: A review, Sensors, 23 (2023) 7863. https://doi.org/10.3390/s23187863
[10]. Y. Cheng, Z. Tian, D. Ning, K. Feng, Z. Li, S. Chauhan, G. Vashishtha, Computer vision-based non-contact structural vibration measurement: Methods, challenges and opportunities, Measurement, 243 (2025) 116426. https://doi.org/10.1016/j.measurement.2024.116426
[11]. C. Z. Dong, F. N. Catbas, A review of computer vision-based structural health monitoring at local and global levels, Structural Health Monitoring, 20 (2021) 692-743.
[12]. H. Nyquist, Certain topics in telegraph transmission theory, Proceedings of the IEEE, 90 (2002) 280-305. https://journals.sagepub.com/doi/10.1177/1475921720935585
[13]. N. Wadhwa, M. Rubinstein, F. Durand, W.T. Freeman, Phase-based video motion processing, ACM Transactions on Graphics, 32 (2013) 1-10. https://doi.org/10.1145/2461912.2461966
[14]. N. Wadhwa, Revealing and analyzing imperceptible deviations in images and videos, Doctoral dissertation, Massachusetts Institute of Technology, Cambridge, MA 02139, United States, 2016.
[15]. S. R. Ibrahim, Random decrement technique for modal identification of structures, Journal of Spacecraft and Rockets, 14 (1977) 696-700. https://doi.org/10.2514/3.57251